

Robotic Friction Stir Welding using a Standard Industrial Robot

Christopher B. Smith
Tower Automotive, Milwaukee, WI

ABSTRACT

In the automotive industry, a barrier to widespread implementation of friction stir welding (FSW) for aluminum joining is the perceived need for high cost, custom capital machinery. The reason for this perception is that the FSW process requires relatively large forces that commonly used automation machinery (e.g. an industrial robot) has difficulty producing. Further complicating the issue, is the need to perform FSW over three-dimensional contours. This further increases the cost of custom capital equipment.

Industrial robots would be a preferred solution for performing FSW for a number of reasons, including; their widespread use in the automotive industry, their ability to repeatedly follow three-dimensional paths, and their low costs. For these reasons, a project was initiated to determine the capability of an industrial robot to perform the FSW process. A FSW system was integrated to an ABB robot. Initially, the robot had little success performing FSW, but welds could be made. The implementation of a force control (rather than position control) strategy greatly improved the results. Three dimensional lap welds (2 mm to 2 mm) have been made at travel speeds between 1 and 2 meters per minute.

This paper will describe the robotic FSW system. In addition, a case study will be explored that involves dissimilar thickness tailor welded blanks, where at least a five-degree of freedom system is necessary to generate welds. High integrity dissimilar thickness butt welds (1 mm to 2 mm) have been made at travel speeds approaching 2 meters / minute.

INTRODUCTION

The FSW process offers significant advantages as compared with fusion joining processes for aluminum, several of which are particularly important to the automotive industry. These advantages include, improved joint efficiency (tensile strength), improved fatigue life, no need for consumables, and improved process robustness. The challenges of the process have included low travel speeds and relatively high force requirements. Although, the travel speeds have been an issue, the travel speeds are now competitive with other fusion joining processes, such as Gas Metal Arc Welding (GMAW). However, the relatively high force requirements of FSW still pose particular challenges for implementation of FSW into the automotive assembly environment, where articulated arm robots are the preferred choice, due to their widespread use and relative low cost.

Although the FSW process requires large forces, it was unknown to what extent an articulated arm robot could perform FSW. Prior to testing, it was the general consensus that a robot would have extremely limited FSW capability. However, because the actual capability was unknown and the cost of alternative machines is at least a factor of ten times that of an articulated arm robot, a project was initiated to investigate performing FSW on an articulated arm robot.

To test the robot's FSW capability, a FSW system was integrated to an ABB IRB 6400 robot. Originally, little success was achieved due to the robot's inherent lack of stiffness. However, the implementation of a force control strategy greatly improved the results.

ROBOTIC SYSTEM DEVELOPMENT

Before integrating the FSW system to an industrial robot, two major decisions were made. The first decision was the type of robot on which to integrate the FSW system. An ABB robot was chosen for its open architecture (high level programming language). This high level language capability would allow for routines to be written to overcome unknown reactions of the robot to the FSW process. As for the specific robot model, the highest payload capacity robot (IRB 6400 -150 kg) was chosen.

The second decision was with regard to the type of system used to rotate the FSW tool. Due to the unknown capability of the robot to perform FSW, minimization of the cost of the rotary power source was important. To meet this constraint, a 2200 W (3 HP) Reliance frequency drive electric motor was chosen. The motor was encased in a housing, on the end of which was a spindle. The spindle transferred the process loads into the housing, rather than the electric motor.

During testing of this system, it was quickly learned that the robotic system's FSW capability was very limited. There were significant problems with excitation of resonance in the robot arm, which caused the entire system to shake violently. Another issue was the robot motors reaching their torque limits. However, on occasion, with the robot in a specific position and orientation, a quality short weld could be made. From this experience, it was concluded that the large size of the motor was a significant problem. The large size of the motor forced the FSW tool to be a significant distance (600 mm) from the wrist of the robot. Given that an articulated arm robot only has revolute joints, the torque required from the robot's motors increases with the distance the tool is from the wrist of the robot. Furthermore, the longer distance allows for easier excitation of resonant motion, i.e., the entire system's mechanical stiffness reduces as the distance from the wrist to the FSW tool increases.



Figure 2: Robotic Friction Stir Welding System

After these initial trials, it was decided that a better solution would be to employ a small hydraulic motor. A hydraulic pump would be used to supply hydraulic fluid to the small motor. The hydraulic motor was also encased in a housing, on the end of which was another spindle. The size of all of this equipment was minimized, due to the previous experience. A 2200 W (3 HP) hydraulic motor with 0 to 3600 RPM range was chosen. A photograph of the system is shown in Figure 2 and a diagram of this system is shown in Figure 3. This system performed much better than the system using the electric motor. Quality welds could be made over a much larger range of the working envelope and robot arm resonance was much less of a problem.

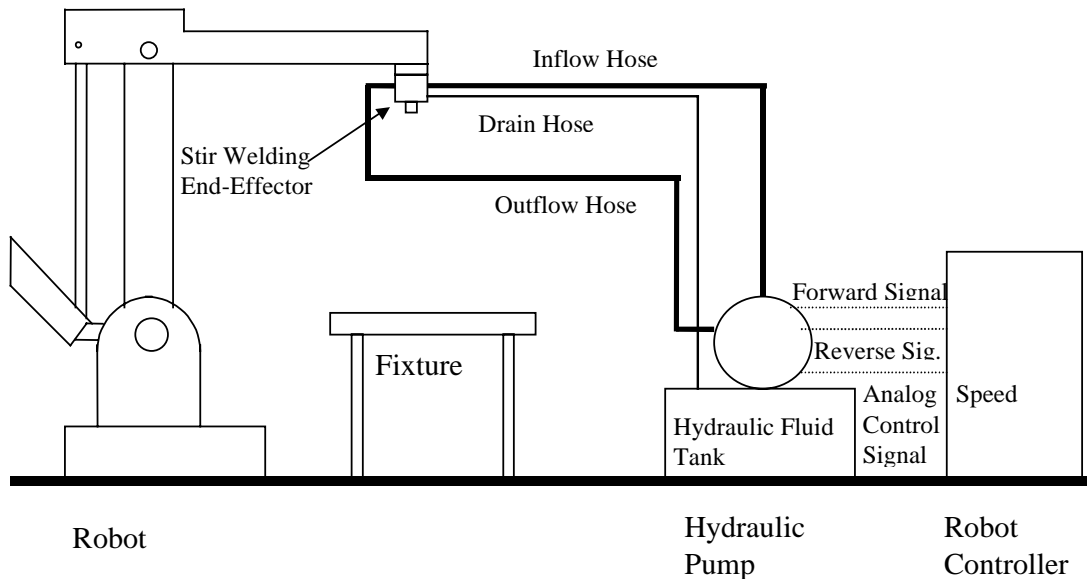


Figure 3: Robotic Friction Stir Welding System Diagram

For the purposes of testing the system, a fixture was fabricated to make 2 mm to 2 mm lap penetration welds in 6061-T6 aluminum. To test the system's capability with this weld configuration, welds were attempted at various travel speeds, rotation speeds, and locations in the working envelope. From this testing, the following conclusions were drawn:

- 1) Only higher rotation speeds could be used (greater than 1500 RPM), otherwise the robot's motors tended to exceed their torque limits
- 2) A travel speed of only 0.6 m / min could be achieved, otherwise the robot's motors tended to exceed their torque limits
- 3) Welds could be made, but only in a limited portion of the working envelope, otherwise there was a tendency to excite a resonant motion in the robot.
- 4) Resonant motion could still be generated, and had the following characteristics. If the plunge of the tool was completed without excitation of resonant motion, the remainder of the welding (traverse) tended to have stable robot motion. Conversely, if resonant motion was observed on the plunge it was often observed throughout the weld path.
- 5) Robot arm deflection of up to 5 mm was observed in the vertical direction. This was compensated for by artificially commanding the robot to plunge below the work piece.
- 6) The hydraulic stir welding motor often stalled, especially at lower rotation speeds. It was apparent the lack of inertia of the hydraulic motor was an issue. Small torque disturbances of the process had a more severe effect on the hydraulic motor with less inertia versus the large electric motor with the same power rating.

From this system, it was apparent that a larger hydraulic motor was necessary, to prevent the motor from stalling when small disturbances were encountered. Furthermore, even though the system performed much better than the first setup, more force capability was necessary. Though it has a lower payload, the ABB Robotics IRB 6400 PE has more force capability than the highest payload robot. With the reduced size of the end-effector, as a result of using the hydraulic motor (lowered total end-effector mass), the lower payload rating of the robot was exceeded. Thus, a new, higher capacity, hydraulic motor and IRB 6400 PE robot were purchased to satisfy these needs.

ROBOTIC FORCE CONTROL

The other challenge that was noted with this system was the deflection of the robot. To overcome this challenge, a force control strategy was implemented. To implement force control, force measurement was necessary. However, additional hardware to measure the force was deemed undesirable, from a cost and maintenance perspective. Fortunately, with the open architecture of the ABB robot, a force measurement system could be implemented in software.

On the ABB robot, the motor torque can be monitored in real time. If one assumes the robot is a rigid body, then equations can be developed for the end of arm force as a function of the motor torques. A multi-tasking routine was written to calculate the end-of-arm force at all times. In this routine, path offsets are calculated using a PID control strategy based on the error between the commanded force and the calculated force. A control diagram for the system is shown in Figure 4.

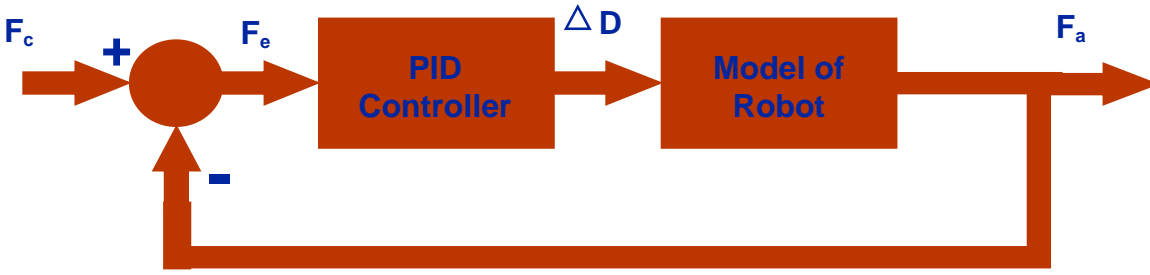


Figure 4: Controller for Robotic FSW Force Control

F_c = commanded force,

F_e = error in force (actual force subtracted from commanded force)

F_a = actual force, as calculated from motor torques

ΔD = commanded robot path displacement

During testing of the force control algorithms, it was determined that a force update rate (sample rate) of only 2 Hz was achievable. This is due to significant computational overhead of the end-of-arm force calculations. With this slow sample rate, implementation of the algorithms was only feasible during the traverse. The high rate of change of the process loads during the tool plunge operation prohibited the use of the force control during plunge of the tool.

To test the force control algorithm, the same 2 mm to 2mm lap penetration welding setup was employed. The sample was fixtured such that it was level. Output from the force control is plotted in Figure 5. The calculated (actual) force is plotted for a condition when the force control was active and another case when the force control was inactive. In addition, the commanded force is overlaid for the case when the force control was active. In both cases, the robot's programmed path was identical. The programmed path had the start point at a vertical position that generated a good weld and the end position was programmed 2 millimeters above the start point. The start of the line indicating the commanded force is coincident with the activation of the force control (start of the traverse). It can be seen that the force control algorithm maintains the desired force during the traverse.

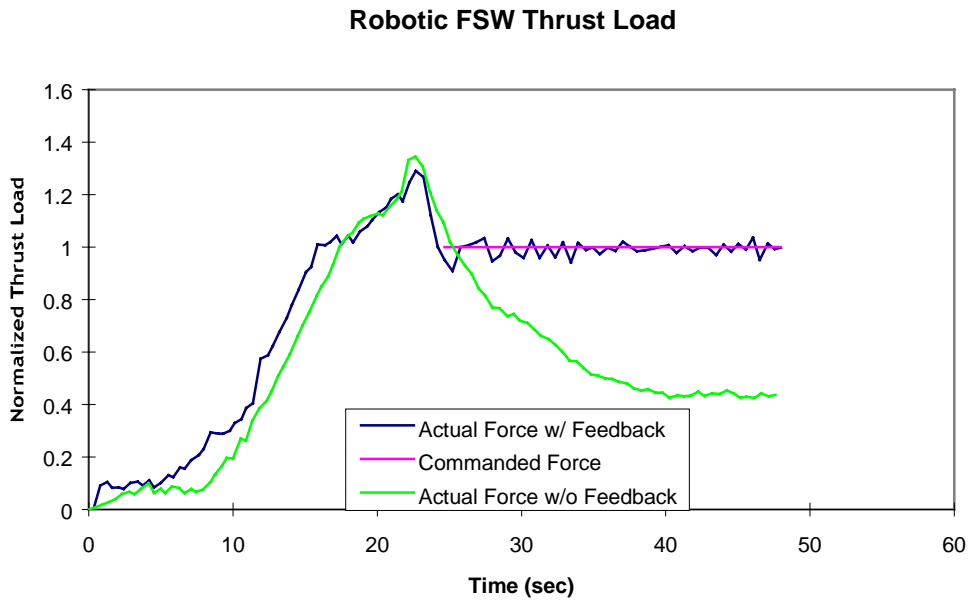


Figure 5: Force Control Output

Sample welds from this testing are shown in Figure 6. It is apparent that the force control algorithm maintained an appropriate force level and yielded a quality weld, whereas the weld without force control active produced a surface void shortly after the start. Of importance is the location of the void initiation of the weld without force control active. From observing the force output, it can be seen that the void does not initiate until the vertical force is approximately 75% of the commanded force.

This apparently explains why force control is an effective tool for controlling the friction stir welding process using a machine that lacks stiffness. When implementing force control, small errors in the actual force versus the commanded force have little effect on the weld quality. From this, it can be concluded that there is a large change in process force between the point of void initiation (vertical position of tool too high) and the point of excessive flash generation (vertical position of tool too low). To the contrary, the range of positions where the same events (i.e. flash generation to void initiation) occur is relatively small (several tenths of a millimeter). This indicates that force control is a more appropriate control strategy than position control, especially in cases where the tool to backing surface distance tolerance is not critical, e.g. lap welds or partial penetration butt welds.

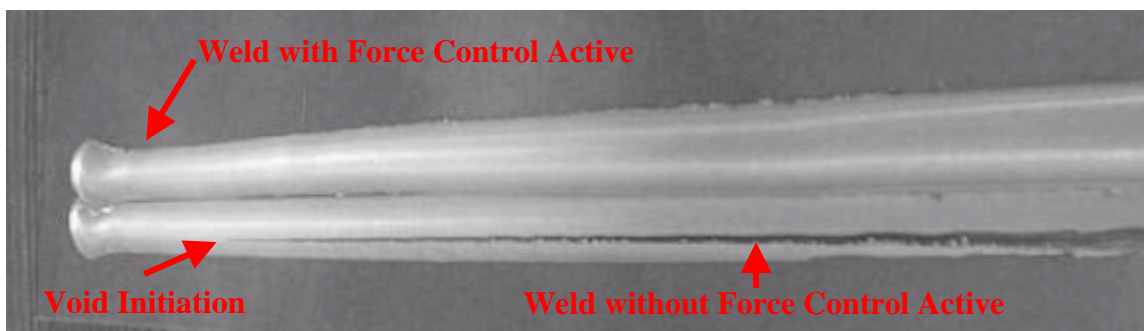


Figure 6: Welds Created with and without Force Control

MULTI-DIMENSIONAL FRICTION STIR WELDING

The main objective of the robotic FSW system was to develop a system for multi-dimensional FSW. After the implementation of the force control system, fixtures and parts were setup to create welds having 2D and 3D contours. To test the robot's ability to create welds along two-dimensional contours, two sections of 6061-T6 2 mm sheet were laid upon one another. This would allow simulation of a lap penetration joint having a 2D contour. A photograph of a completed 2 mm to 2 mm lap penetration weld on a 2D contour is shown in the Figure 7A.

A fixture and parts were also fabricated to test the robot's capability of producing stir welds along three-dimensional paths. The fixture was setup for joining of 2 mm to 2 mm material. The path started on a 10° downward angle for 100 mm, followed by a 45° arc (75 mm radius), and was completed after a 55° downward angle for approximately 100 mm. The 2 mm aluminum sheets were crudely secured to the fixture with vice grips and C-clamps. A photograph of the setup is shown in the right side of Figure 7.

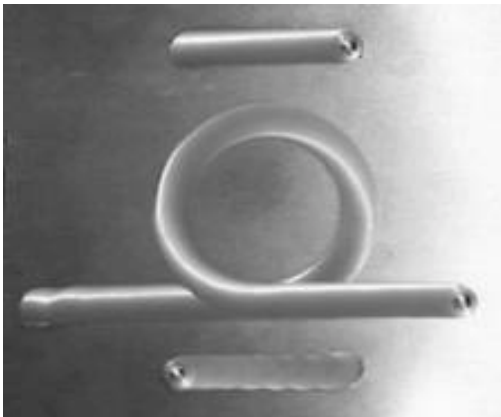


Figure 7A: 2D Robotic FSW



Figure 7B: 3D Robotic FSW

CASE STUDY: ROBOTIC FSW OF TAILOR WELDED BLANKS

One application in the automotive industry where FSW will offer significant advantages, where at least a 5 degree of freedom machine will be required, is the aluminum tailor welded blank (TWB). A purpose of the TWB is to reduce the weight of stamped components. This is accomplished by reducing the material thickness in sections of stampings, where the strength requirements are reduced. Varying alloy combinations may also be present in certain blanks, especially in cases where the degree of forming varies significantly over portions of the blank. A diagram depicting possible TWB geometries is shown in Figure 8.

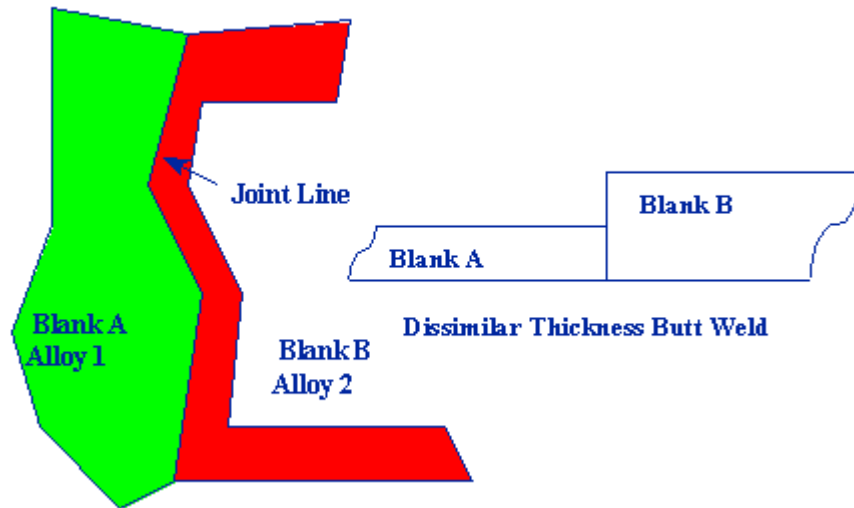


Figure 8: Tailor Weld Blank Geometry

To test the feasibility of applying FSW to the aluminum TWB application, a FSW robotic system was employed. In the study, 1 mm material was joined to 2 mm material of various alloys. The alloys included 6061-T6, 5754-O, and 6111-T4, however both blanks were always of the same alloy. The weld joints investigated are shown in Figure 9. Early research indicated that welds made from the similar thickness side (Figure 9A), produced results that did not meet expectations. The reason for this was that welds made from this side resulted in a notched transition from the thin to the thick side of the joint that caused a stress concentration. Thus, all future welds were made from the dissimilar thickness side, as indicated in Figure 9B.



Figure 9A: Similar Thickness Side TWB Figure 9B: Dissimilar Thickness Side TWB

For FSW of the dissimilar thickness butt joint geometry, many unknowns surface, including:

- 1) Tool design. Tool designs used for similar thickness butt welds may not be appropriate. Specifically, the tool pin length and shoulder diameter are unknown and changes in them can have significant consequences in this process.
- 2) Travel angle and work angles. These are indicated in Figure 10 and are described similarly in the GMAW process. The work angle is the orientation of the tool about the axis of travel and the travel angle is the orientation of the tool about the axis that is perpendicular to the travel direction.
- 3) Rotation speed.
- 4) Travel speed.
- 5) Rotation direction, especially with non axi-symmetric tools.
- 6) Relative orientation of the thin and thick material, especially with non axi-symmetric tools.

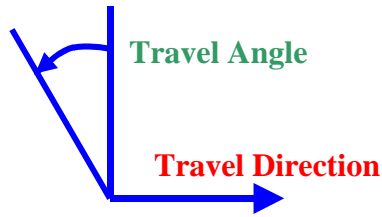


Figure 10A: Travel Angle

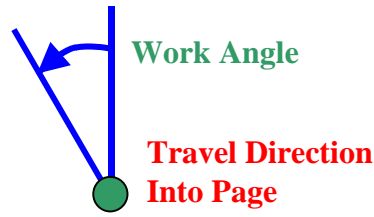


Figure 10B: Work Angle

It is important to note that the tool design process for the dissimilar thickness blank must be an iterative process, until a data base of tool designs has been established. Assuming that a tool of a known shoulder diameter is going to be used, the optimal travel and work angles are unknown. That is, some work must be done to develop appropriate work and travel angles. Once the optimal travel and work angles are determined, then and only then, can the pin length be determined. It is noted that the effective location of the pin tip is affected by changes in these angles.

Some general observations about parameters have been made with regard to the welding of dissimilar thickness joints. In Figure 11 and Figure 12, results of inappropriate work and travel angles are diagramed. Generally, if the work angle was too large, then thinning resulted on the thin material side and excessive flash was generated on the thick material side. This is indicated on the left in Figure 11. However, if the work angle was too small, then poor bonding was produced on the thin material side and undercut was possible on the thick material side. As for the travel angle, it was observed that small travel angles produced a digging effect, where the front of the tool was below the corner of the thicker material. This is indicated in Figure 12. Large travel angles generally result in excessive flash on both the thin and thick material side, as well as increase the vertical force.

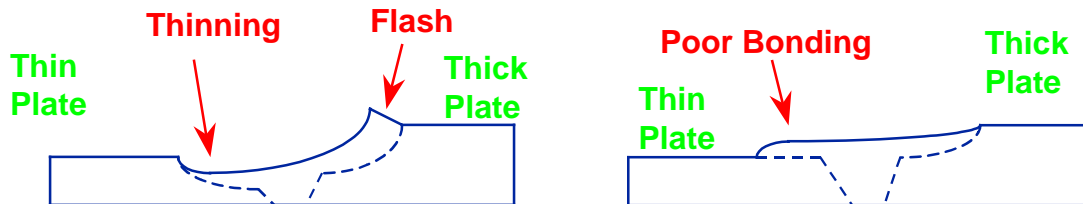


Figure 11: Problems Associated with Incorrect Work Angle

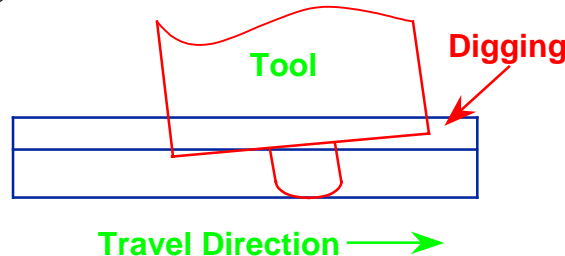


Figure 12: Problems Associated with Incorrect Travel Angle

From our observations, flash generation appears to be the most difficult problem to overcome in the FSW of TWB application. Flash can be generated on both the thin and thick sides, as well as

extruded out from the underneath the tool. The flash that extrudes out from underneath the tool, extrudes out front from the leading edge of tool at a rate higher than the travel speed and does not adhere to the material. It has also been observed that at higher travel speeds, elimination of flash is more difficult. However, flash generation can be eliminated through proper selection of all parameters, including tool design.

During the parameter development phase, special emphasis was placed on optimizing the travel speed. With no consumables and little maintenance cost, the operating cost of the FSW process is highly dependent on travel speed. Travel speeds up to 1.8 meters/minute were achieved. At travel speeds of 1.8 m/min, FSW can be competitive with any process that currently joins 1 mm to 2mm 5xxx and 6xxx aluminum. However further increases in travel speed are probably achievable, to further decrease the cost of the FSW operation.

After achieving welds of good visual quality at the high travel speeds, metallography, tensile testing, and bend testing was performed on the welds. A cross-section of one of the welds is shown in Figure 13. A trace of the original oxide layer appears to be present near the center of the weld. Pull testing of these welds resulted in failures near the center-line of the weld or in the heat affected zone for the 6xxx welds. Welds in the 5xxx series that were tensile tested resulted in failures in the parent metal, but root openings appeared to be present. For the bend tests, a 12.5 mm diameter mandrel was used. The welds passed the face bend tests, but failed the root bend test. All of this indicated that there was incomplete penetration. For the original tool, a pin length of the average thickness (1.5 mm) was chosen. After doing the geometrical analysis, using the shoulder diameter, travel angle, and work angle used to create these welds, it was apparent the pin length was not sufficient.

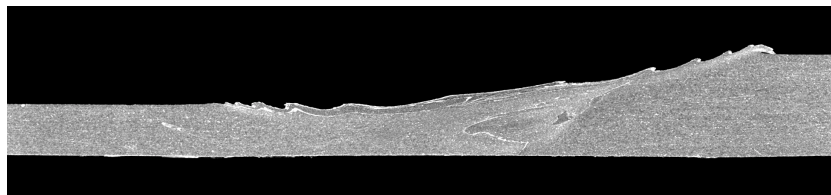


Figure 13: Weld Cross-Section (1mm to 2mm 6061-T6)

To overcome this problem, the pin length was increased. A new tool was fabricated and the testing was repeated. This time, the results were much improved. A photograph of the 6111 and 5754 samples that were tensile tested is shown in Figure 14. Based on the thinner material, the joint efficiencies were 100% for the 5xxx series and approximately 80% for the 6xxx series. The 6xxx series welds failed at the edge of the stir zone on the top side of the weld and through the heat affected zone on the root side. The failure location is likely at the root of one of the ripples on the top surface of the weld (see Figure 13). At the root of the ripple, the effective material thickness has been reduced.



Figure 14: Weld Cross-Section (1mm to 2mm 6061-T6)

CONCLUSIONS

- 1) It is possible to perform FSW with a standard industrial robot on Aluminum 6061-T6 up to 3 mm in thickness.
- 2) Force control is a critical component to the success of FSW with an industrial robot. A robot with an open architecture is required to implement force control.
- 3) Force control allows the machine to overcome inherent lack of stiffness and to repeatedly position the tool vertically with respect to the weld joint line.
- 4) The force control update rate of 2Hz is too slow for use on the plunge operation. Improvements in robot computation performance are needed.
- 5) Smaller deflections transverse to weld direction must be overcome by artificially offsetting program positions, similar to what was done with early arc welding robots.
- 6) Although FSW can be performed with an industrial robot, increases in stiffness would improve the applicability of industrial robots to the FSW process.
- 7) The industrial robot is ideal for the aluminum tailor welded blank application due to the 5 degree of freedom motion requirements of the application and the relatively thin material. If a robot were not used, then expensive flexible fixturing would be required to generate the work and travel angles required for the process.
- 8) Robotic FSW of aluminum tailor welded blanks is feasible at nearly 2 m / min travel speeds, making FSW a very cost competitive process, in addition to bringing all of the other benefits of the process to the application.

REFERENCES

- 1) Broman, R. E., Smith, C. B., Noruk, J. S., and McDonald, W. M., Challenges of Robotic Welding of Aluminum Structures, Proceedings of the 38th Conf. Of Metallurgists, August 1998.
- 2) Thomas, W.M. et al, Friction Stir Butt Welding, U. S. Patent No. 5,460,317.
- 3) Dawes, C. J. and Thomas, W. M. Friction Stir Process Welds Aluminum Alloys, Welding Journal. Volume 75, March 1996, Pg. 41-45.
- 4) Smith, C.B., Robotic Friction Stir Welding: Phase I Initial Feasibility Study, Report APPT-1493, Tower Automotive Internal Report, May 1997.
- 5) Smith, C.B., Robotic Friction Stir Welding: Phase II Robot Performance Comparison, Report APPT-1494, Tower Automotive Internal Report, May 1998.

- 6) Smith, C.B., Robotic Friction Stir Welding of Tailor Welded Blanks, Report ATP-1536, Tower Automotive Internal Report, April 2000.
- 7) Peters, R.S., Formed Aluminum Tailor Welded Blanks, Report APPT-1509, Tower Automotive Internal Report, June 1998.